FORECAST VALIDATION OF THREE SIERRA NEVADA PRECIPITATION EVENTS

Rebekah I.Banas[1], Heather Dawn Reeves

National Weather Center Research Experiences for Undergraduates

and

Central Michigan University

National Severe Storms Laboratory

University of Oklahoma, Norman, Oklahoma

Cooperative Institute for Mesoscale Meteorological Studies

University of Oklahoma, Norman, Oklahoma

ABSTRACT

In this paper, three precipitation events which occurred in the Sierra Nevada Mountains are investigated. These three events are all associated with atmospheric rivers, from which the resulting precipitation can be quite heavy. The 24-, 48-, and 72-h NAM model forecasts of temperature, dewpoint, and 24-h accumulated precipitation are analyzed at four Sierra Nevada stations. Temperature and dewpoints errors from the model output show a tendency to overestimate the temperature and underestimate the dewpoint during these three events. For one event, the precipitation was strongly underestimated (by about half). The other two events show no specific trend in either time or space.

1. INTRODUCTION

Precipitation in the Sierra Nevada Mountains of California can be quite heavy sometimes, leading to flash floods and landslides. Thus, accurate forecasts of the precipitation amount and type are very important for local emergency managers and dam operators. These precipitation events are often associated with atmospheric rivers, which are horizontal elongated regions of enhanced moisture transport (Ralph et al. 2004). Although loosely defined as above, atmospheric rivers may have considerable case-to-case variability. Some of the observed differences

[1] Rebekah I. Banas
6435 Cronk Rd
Corunna, MI 48817
beckybanas@hotmail.com

among river events include: the cross-stream river width, the amount of moisture transport, and/or the height of the freezing level (Reeves et al. 2008; Jankov et al. 2009; Lundquist et al. 2008). These variations may lead not only to different precipitation patterns but also to differing levels of forecast accuracy. Here, three case studies, with different atmospheric rivers, are analyzed in an attempt to find patterns or trends in the model output.

Heavy precipitation in California most often occurs in winter in association with so-called atmospheric rivers (Ralph et al. 2004). Atmospheric rivers are formally defined as a narrow, elongated plume of integrated water vapor (IWV) equal to or exceeding two centimeters (IWV ≥ 2 cm) (Ralph et al. 2004). As the moisture laden air is forcibly lifted along the western faces of the Coastal Ranges and Sierra Nevada mountains (Fig. 1), water vapor is converted to precipitate, sometimes leading to very high accumulations (Neiman et al. 2002; James et al. 2005). In the past six years, there have been 117 atmospheric rivers which impacted the California coast, according to ongoing records provided by NOAA ESRL (Earth Science Research Lab) (P. Neiman, personal communication). Yet, not all atmospheric rivers are associated with heavy precipitation. Additionally, not all heavy precipitation events are due to atmospheric rivers. In the past six winter seasons there have been 337 events in which the 24-hour accumulated precipitation exceeded 38 mm; of these, 273 events are not associated with atmospheric rivers. Also within the same time period, there have been 125 events in which the 24-hour accumulated precipitation exceeded 76 mm.

Within the broader definition of atmospheric rivers provided above, there is potentially important variability that may affect the type and amount of precipitation. For example, such variability includes: the horizontal gradient of moisture within the airmass (Rotunno and Ferretti 2001), the horizontal configuration of the static stability of the airmass (Galewsky and Sobel 2005), the cross-stream width of the moisture stream with respect to topography (Reeves et al. 2008), the alteration of the precipitation distribution with respect to the height of the melting level (Jankov et al. 2009), and the strength of the orographic precipitation gradient (OPG) with respect to precipitation types (Lundquist et al. 2010). These forms of variability and others lead one to question whether there is also variability in the accuracy of numerical model forecasts. What kinds of errors are present in the forecasts for these river events? Does a particular kind of event have a better forecast? Is it really the case that the forecasts worsen as lead time increases?

In this paper, three case studies are selected for analysis. Each case has a different river and differing amounts of precipitation associated with it. Output from the North American Mesoscale model (NAM; Janjic et al 2005) are compared to available observations for each case.

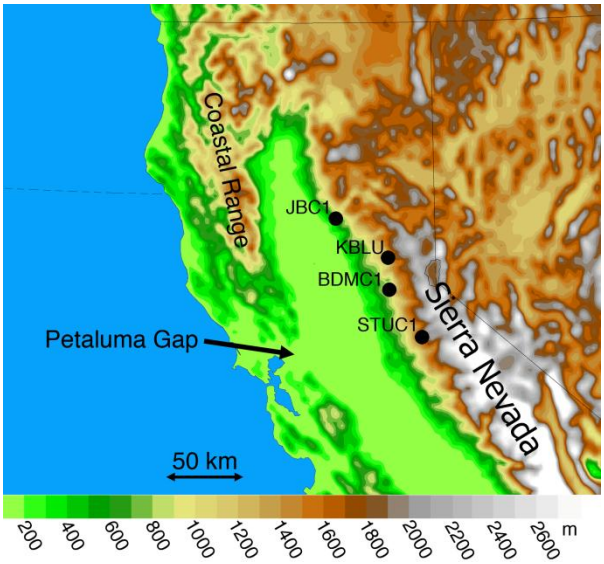

Fig (1) Locations of four Sierra Nevada stations

2. THREE CASE STUDIES

a. 25 October 2010
The 25 October 2010 event is characterized by a broad atmospheric river and heavy precipitation. The river has two forks which converge to impinge upon almost the entire California coast by the evening of 24 October (Fig. 2a). The

atmospheric river has a predominantly zonal flow and a core maximum value of IWV ≥ 45 mm. The 24 hour accumulated precipitation ending at 12Z on 25 October has a maximum value of 203 mm (Fig. 3a). [The precipitation estimates are provided by Advanced Hydrologic Prediction Service (AHIPS).] This precipitation maximum is located on the crest of the Sierra Nevadas north of the Petaluma Gap. Based upon hourly rain gauge observations from 12Z on the 24th to 12Z on the 25th, the time of maximum precipitation accumulation was at approximately 18Z on 24 October.

b. 9 December 2010
The 9 December 2010 event is characterized by a narrow atmospheric river and a relatively low amount of precipitation. The river impinges upon the northern California coast just north of the Petaluma Gap (Fig. 2b). The atmospheric river has principally zonal flow and a core maximum value of IWV ~ 40 mm. The 24 hour accumulated precipitation ending at 12Z on 9 December has a maximum value of 51 mm (Fig. 3b). This precipitation maximum is located on the crests of the northernmost Sierra Nevadas. Hourly rain gauge observations from 12Z on the 8th to 12Z on the 9th indicate that the time of maximum precipitation accumulation was at approximately 15Z on 8 December.

c. 8 November 2010
The 8 November 2010 event is characterized by a somewhat narrow atmospheric river and a moderate amount of precipitation. The river impinges upon the northern California coast (Fig. 2c). The atmospheric river has meridional flow and a core maximum value of IWV ~ 40 mm. The 24 hour accumulated precipitation ending at 12Z on 8 November had a maximum value of 102 mm (Fig. 3c). This precipitation maximum is located on the western faces of the Sierra Nevadas north of the Petaluma Gap. Rain gauge observations indicate that the time of maximum precipitation accumulation was at approximately 15Z on 7 November.

a.

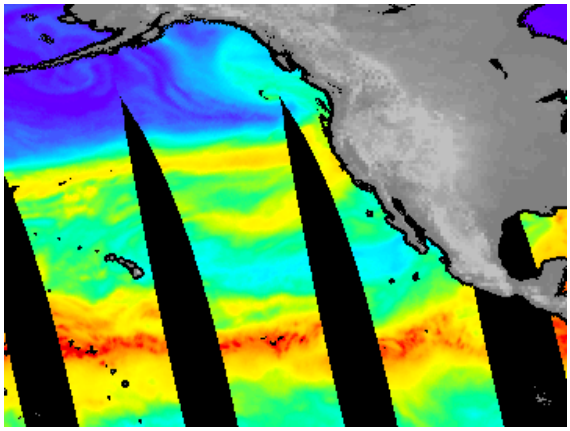

b.

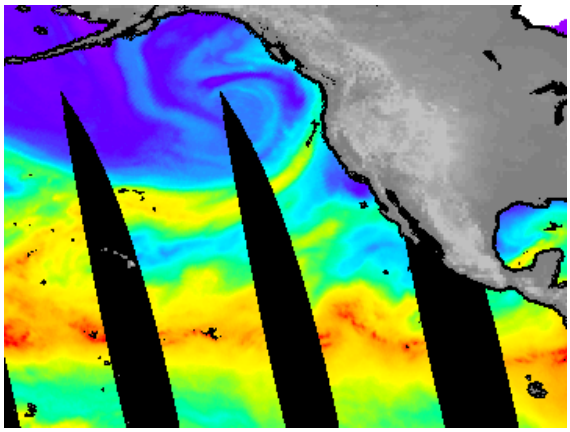

c.

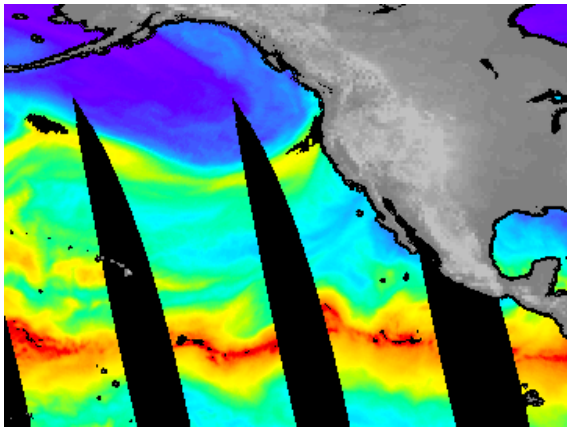

Fig (2) SSM/I satellite imagery of IWV for **(a)** 24 Oct 2010 **(b)** 8 Dec 2010 **(c)** 7 Nov 2010

a.

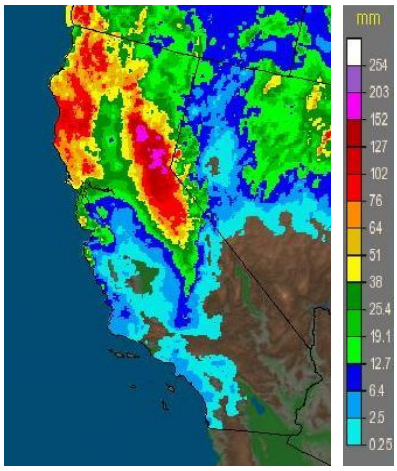

b.

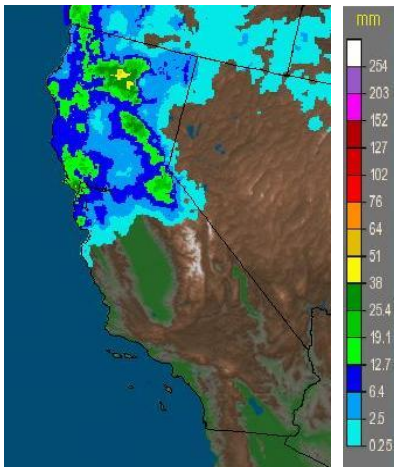

c.

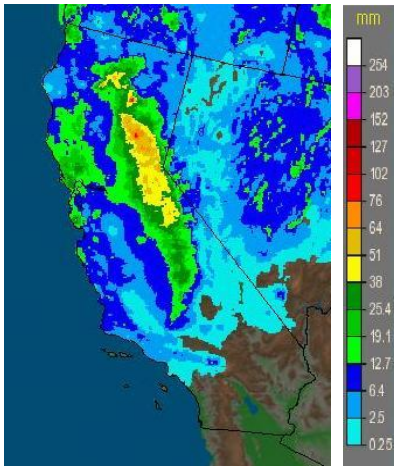

Fig (3) AHIPS 24-h precip accumulations for **(a)** 24 Oct 2010 **(b)** 8 Dec 2010 **(c)** 7 Nov 2010

3. METHODS

a. NAM Model

The forecasts are analyzed for these three events and are output from the NAM model, which is produced using the Weather Research and Forecasting Non-Hydrostatic Mesoscale Model (WRF-NMM; Janjic et al. 2005). The NAM model has a horizontal grid spacing of 12 km and includes 60 terrain-following vertical levels. It is initialized each day at 0000, 0600, 1200, and 1800 UTC. The NAM's initial conditions are produced by combining the 12-hr forecast from the global forecast model with certain assimilated variables. These variables include aircraft, satellite, surface, and upper-air observations which are incorporated via use of a three-dimensional variational-analysis scheme. The NAM model uses the following schemes: the Ferrier microphysical (Ferrier 1994), the Betts-Miller-Janjic cumulus (Betts and Miller 1986; Janjic 1994), and the Geophysical Fluid Dynamics Laboratory longwave and shortwave radiation (Fels and Schwarzkopf 1975; Ramaswamy and Freidenrich 1998). This model parameterizes the boundary layer using the MYJ scheme and also utilizes the Noah land surface model (LSM; Ek et al. 2003). In addition, the NAM model takes into consideration the effects of orographic shading in the shortwave radiation scheme and for sloped terrain uses a one-sided horizontal diffusion.

b. Station list and variables used in analysis

The observations for the three case studies are taken from RAWS (Remote Automated Weather Stations) and NWS (National Weather Service) stations in the Sierra Nevada mountains. All the stations are located north of the Petaluma Gap. The locations include: BDMC1 (Bald Mountain), JBGC1 (Jarbo Gap), KBLU (Emigrant Gap, Blue Canyon), and STUC1 (Cottage).

The variables that will be used in the analysis include: the 2-m temperature and dewpoint, the 10-m winds, and the 24-hour precipitation measurements.

c. Statistical method

The output from the NAM model is extracted for each of the stations listed above for a 24 hour period surrounding the time of max precipitation for each of the three case studies. The model data are interpolated to the latitude and longitude of the observation sites using the inverse-distance Cressman method,

$$T = \frac{\sum_{n=1,4} W_n T_n}{\sum_{n=1,4} W_n} \quad , \qquad (1)$$

where T_n is the 2-m temperature or dewpoint at the four model grid points surrounding the observation site and W_n is a weight given by,

$$W_n = \frac{R^2 - D_n^2}{R^2 + D_n^2} \quad . \qquad (2)$$

In (2) R is the horizontal grid distance of the model (12 km for the NAM) and D is the distance from the grid point to the observation site (Cressman 1959).

The forecasted 2-m temperatures and dewpoints and the magnitude of the 10-m wind are quantitatively compared with the observations from each station.

Additionally, a percent error is calculated for the 24, 48, and 72 hour precipitation forecasts for each of the three events. This percent error was calculated as follows,

$$\%\ error = \frac{P_{fcst} - P_{obs}}{P_{obs}} \qquad (3)$$

where, P_{fcst} is the forecasted amount of precipitation (mm) for a station and P_{obs} is the amount of observed precipitation at that same site.

4. RESULTS

a. 25 Oct 2010

At each of the four stations, the precipitation is underestimated for all forecast lead times by 30-80 mm (Fig. 5a). BDMC1 and STUC1 have the largest errors, with the precipitation being underestimated by 46% to 50%. At KBLU, the precipitation is underestimated by 22% to 25%. At JBGC1, the precipitation is underestimated by 16% to 33%.

The temperature and dewpoint errors are calculated and plotted for the 24-, 48-, and 72-h forecasts at these four stations (Fig. 6a) for a 24-h period surrounding the time of heaviest precipitation. The model has a tendency to overestimate the temperature at all lead times. But, KBLU has an episode where the temperature is overestimated (18Z 24 Oct and 00Z 25 Oct). Conversely, the dewpoint temperature is underestimated by the 24, 48, and 72-h forecasts at all four stations throughout the 24-h period with one exception. This slight overestimate (0.24 K) occurs during the 24-h BDMC1 forecast at 06Z 25 Oct 2010.

b. 9 Dec 2010

Unlike 25 Oct 2010, there is no clear trend in the precipitation forecasts for this event (Fig. 5b). The lead times range from under- to overestimation. At KBLU, the 24-h precipitation is overestimated for all lead times. Notice that the 72-h forecast is the most comparable to the observations, with an overestimate of 4 mm (26%). During the 24-h and 48-h forecasts, the precipitation is overestimated by 19 mm (121%) and 10 mm (64%), respectively. At JBGC1, the 24-h precipitation is underestimated by 8

mm (38%) and the 48-h and 72-h forecasts overestimate the precipitation by 18 mm (89%) and 3 mm (15%), respectively. At STUC1, the 48-h and 72-h forecasts underestimate the precipitation by 6 mm (31%) and 7 mm (34%), respectively. The 24-h forecast best approximates the observed precipitation at STUC1, with an underestimate of 1.5 mm (8%). At BDMC1, the 24-h forecast overestimates the precipitation by 8.9 mm (85%), and the 48-h and 72-h forecasts underestimate the precipitation by 0.1 mm (1%) and 5 mm (51%), respectively.

The temperature and dewpoint errors are calculated and plotted for the 24-, 48-, and 72-h forecasts at these four stations for a 24-h period surrounding the time of heaviest precipitation (Fig. 6b). There is a similar trend to the 25 Oct 2010 event. The model has a warm bias of forecast temperatures for all lead times as compared to the observations with a few exceptions. There is a slight underestimate (-0.5 to -1.1 K) of temperature at KBLU (18Z 8 Dec and 00Z 9 Dec for the 24-h and 72-h forecasts, 00Z 9 Dec for the 48-h forecast). At JBGC1, the dewpoint is underestimated for all lead times. KBLU also shows this underestimate of the dewpoint with two exceptions. The dewpoint is overestimated on 12Z 24 Oct by both the 48-h (.75 K) and 72-h (2.5 K) forecasts. At STUC1, the dewpoint is overestimated or has a near-zero error (except for 12Z 24 Oct in 24-h forecast). For BDMC1, the dewpoint tendency varies among the lead times. There is a cold bias throughout the 48-h forecast, a cold (12Z 24 Oct to 00Z 25 Oct) and a warm bias (06-12Z 25 Oct) in the 24-h forecast, and a warm (12Z 24 Oct to 00Z 25 Oct) and cold bias (06-12Z 25 Oct) in the 72-h forecast.

c. 8 Nov 2010

As in 9 Dec 2010, the precipitation forecasts do not show a specific trend (Fig. 5c). At STUC1, the precipitation is overestimated for all lead times. The 24-h forecast overestimates by 0.3 mm (0.7%), the 48-h by 30 mm (71%), and the 72-h by 9 mm (20%). At JBGC1, the precipitation is underestimated for all lead times. The 24-h forecast underestimates by 11 mm (19%) and the 48- and 72-h underestimate by 10 mm (17%). At BDMC1, the 24- and 72-h forecasts underestimate the precipitation by 8 mm (15%) and 10 mm (19%), respectively, and the 48-h overestimates by 4 mm (8%). At KBLU, the 24- and 72-h forecasts underestimate the precipitation by 12 mm (19%) and 3 mm (5%), respectively, and the 48-h overestimates by 10 mm (16%).

The temperature and dewpoint errors are calculated and plotted for the 24-, 48-, and 72-h forecasts at these four stations for a 24-h period surrounding the time of heaviest precipitation (Fig. 6c). The model tends to overestimate the temperature for all lead times (except for KBLU 18Z 7 Nov to 00Z 8 Nov). In contrast, the dewpoint is underestimated for all lead times at KBLU, STUC1, and JBGC1 (except for 06Z 8 Nov, overestimate of 0.3-0.6 K). At BDMC1, the 48- and 72-h forecasts underestimate the dewpoint and the 24-h has a cold (06-12Z 7 Nov, 06Z 8 Nov) and a warm bias (18Z 7 Nov to 00Z 8 Nov).

a.

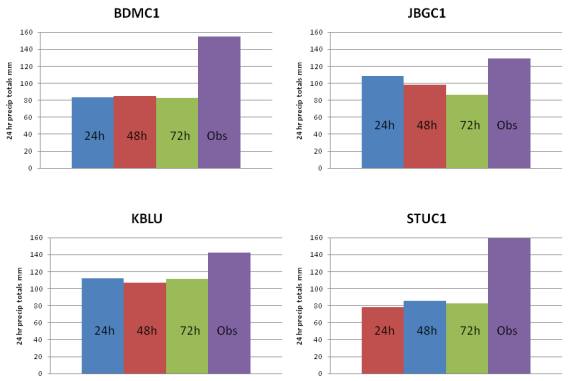

b.

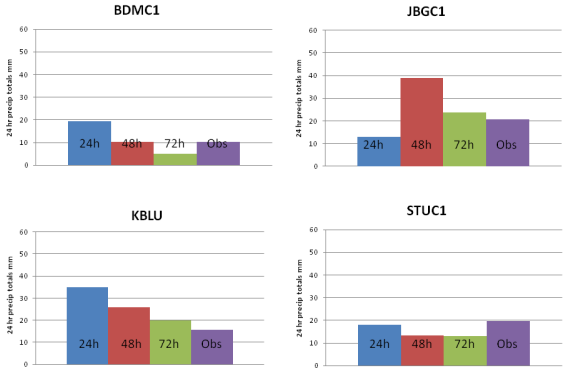

c.

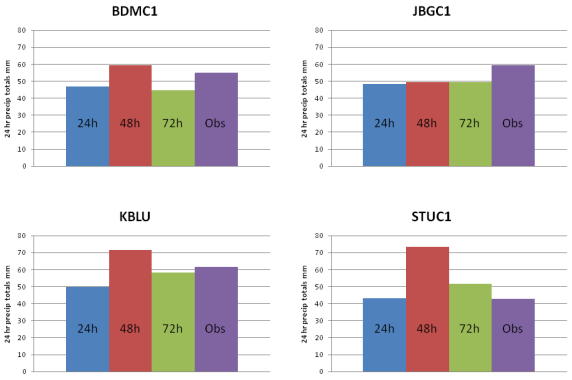

Fig (5) 24-h precipitation accumulations for **(a)** 24 Oct 2010 **(b)** 8 Dec 2010 **(c)** 7 Nov 2010

a.

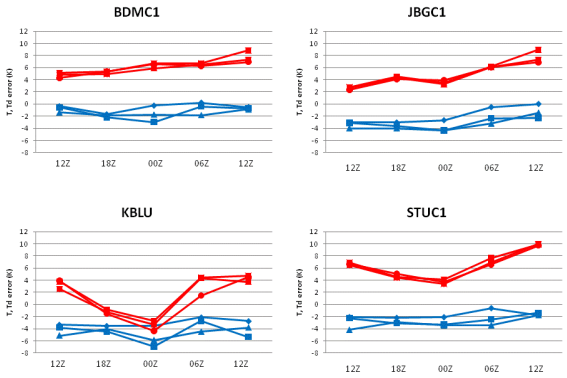

b.

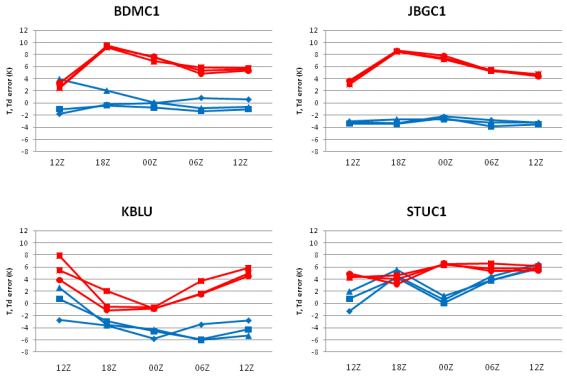

c.

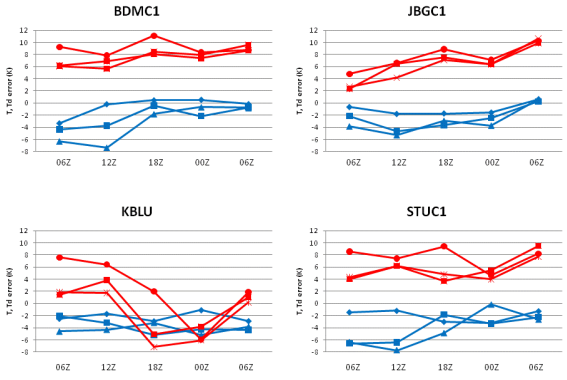

Fig (6) Temperature (red) and dewpoint (blue) errors at the four stations for **(a)** 24 Oct 2010 **(b)** 8 Dec 2010 **(c)** 7 Nov 2010

5. CONCLUSIONS

When comparing the three case studies as a whole, some general traits become evident. The model has a tendency to overestimate the temperature at the four stations during all three events. The model also has a contrasting tendency to underestimate the dewpoint. There are exceptions to both these tendencies, but these general trends result in the model underestimating the relative humidity. This underestimate of RH is likely linked to the underestimate of precipitation.

Although not always the case, the forecasts tend to agree more with each other than with the observations. This suggests that the error does not increase with time and that there is no significant loss of predictability as the lead time increases from 24- to 72-h. There is less agreement between the 24-, 48-, and 72-h forecasts for the 8 Nov 2010 event than with the 25 Oct and 9 Dec events. This could suggest that events similar to the 8 Nov case are more difficult for the model to accurately represent, however, a more rigorous and in-depth investigation would be required to discover if this is a legitimate claim. Another point of interest is that there are differing amounts of precipitation, even though the large scale flow is similar. Considering that the four stations are at different altitudes, an interesting question is raised. Is it the case that the magnitude of error increases with the station altitude? Are the forecasts worse at the higher elevation stations versus those with lower altitude? Although interesting, this question is outside the scope of this work and would require a more thorough investigation to uncover any possible relationships that may exist between the magnitude of error and the station elevation.

6. ACKNOWLEDGEMENTS

The authors gratefully acknowledge: Paul J. Neiman, AHIPS, SSM/I, and Mesowest for the use of archived station data.

This work was prepared by the authors with funding provided by National Science Foundation Grant No. AGS-1062932 and NOAA/Office of Oceanic and Atmospheric Research under NOAA-University of Oklahoma Cooperative Agreement #NA08OAR4320904, U.S. Department of Commerce. The statements, findings, conclusions, and recommendations are those of the author(s) and do not necessarily reflect the views of the National Science Foundation, NOAA, or the U.S. Department of Commerce.

7. REFERENCES

Betts, A. K., M. J. Miller, 1986: A new convective adjustment scheme. Part II: Single column tests using GATE wave, BOMEX, ATEX and arctic air-mass data sets. *Quarterly J. Royal Meteor. Society*, **112**, 693-709.

Cressman, G., 1959: An operational objective analysis system. *Mon. Wea. Review*, **87**, 367-374.

Ek, M., K. E. Mitchell, Y. Lin, E. Rogers, P. Grunmann, V. Koren, G. Gayno, J. D. Tarpley, 2003: Implementation of the Noah land surface model advances in the National Centers for Environmental Prediction operational Mesoscale Eta Model. *J. Geophys. Res.*, **108**, 8851.

Fels, S. B., M. D. Schwarzkopf, 1975: The simplified exchange approximation – A new method for radiative transfer calculations. *J. Atmos. Science*, **32**, 1475-1488.

Ferrier, B. S., 1994: A double-moment multiple-phase four-class bulk ice scheme. Part I: Description. *J. Atmos. Science*, **51**, 249-280.

Galewsky, J., A. Sobel, 2005: Moist Dynamics and Orographic Precipitation in Northern and Central California during the New Year's Flood of 1997. *Mon. Wea. Review*, **133**, 1594-1612.

James, C. N., R. A. Houze, 2005: Modification of Precipitation by Coastal Orography in Storms Crossing Northern

California. *Mon. Wea. Review*, **133**, 3110-3131.

Janjic, Z. I., 1994: The step-mountain Eta coordinate model: Further developments of the convection, viscous sublayer, and turbulence closure schemes. *Mon. Wea. Review*, **122**, 927-945.

Janjic, Z. I.,T. L. Black, M. E. Pyle, H.-Y. Chuang, E. Rogers, G. J. DiMego, 2005: The NCEP WRF-NMM core. Preprints, *2005 WRF/MM5 User's Workshop*, Boulder, CO. CD-ROM, 2.9.

Jankov, I., J.-W. Bao, P. J. Neiman, P. J. Schultz, H. Yuan, A. B. White, 2009: Evaluation and Comparison of Microphysical Algorithms in ARW-WRF Model Simulations of Atmospheric River Events Affecting the California Coast. *Journal of Hydrometeorology*, **10**, 847-870

Lundquist, J. D., P. J. Neiman, B. Martner, A. B. White, D. J. Gottas, F. M. Ralph, 2008: Rain versus Snow in the Sierra Nevada, California: Comparing Doppler Profiling Radar and Surface Observations of Melting Level. *Journal of Hydrometeorology*, **9**, 194-211

Lundquist, J. D., J. R. Minder, P. J. Neiman, E. Sukovich, 2010: Relationships between Barrier Jet Heights, Orographic Precipitation Gradients, and Streamflow in the Northern Sierra Nevada. *Journal of Hydrometeorology*, **11**, 1141-1156.

Neiman, P. J., F. M. Ralph, A. B. White, D. E. Kingsmill, P. O. G. Persson, 2002: The Statistical Relationship between Upslope Flow and Rainfall in California's Coastal Mountains: Observations during CALJET. *Mon. Wea. Review*, **130**, 1468-1492.

Ralph, F. M., P. J. Neiman, G. A. Wick, 2004: Satellite and CALJET Aircraft Observations of Atmospheric Rivers over the Eastern North Pacific Ocean from CALJET-1998 and PACJET-2001: Mean Vertical-Profile and Atmospheric River Characteristics. *Mon. Wea. Review*, **133**, 889-910.

Ramaswamy, V., S. M. Freidenrich, 1998: A high-spectral resolution study of the near-infrared solar flux disposition in clear and overcast atmospheres. *J. Geophys. Res.*, **103**, 23255-23273.

Reeves, H. D., Y.-L. Lin, R. Rotunno, 2008: Dynamic Forcing and Mesoscale Variability of Heavy Precipitation Events over the Sierra Nevada Mountains. *Mon. Wea. Review*, **136**, 62-77

Rotunno, R., R. Ferretti, 2001: Mechanisms of Intense Alpine Rainfall. *Journal of Atmos. Science*, **58**, 1732-1749.